Available online at www.sciencedirect.com
ScienceDirect
Journal of Molecular Structure 874 (2008) 178–186
Journal of MOLECULAR STRUCTURE
www.elsevier.com/locate/molstruc

Synthesis, spectroscopic study, X-ray crystallography and *ab initio* calculations of the two new phosphoramidates: $C_6H_5OP(O)(NHC_6H_{11})_2$ and $[N(CH_3)(C_6H_{11})]P(O)(2\text{-}C_5H_4N\text{-}NH)_2$

Khodayar Gholivand [a,*], Carlos O. Della Védova [b,c,*], Mauricio F. Erben [b],
Hamid Reza Mahzouni [a], Zahra Shariatinia [a], Shadi Amiri [a]

[a] *Department of Chemistry, Tarbiat Modarres University, P.O. Box 14115-175, Tehran, Iran*
[b] *CEQUINOR (UNLP-CONICET), Departamento de Química, Facultad de Ciencias Exactas, Universidad Nacional de La Plata, C.C. 962 (B1900AJL), La Plata, Buenos Aires, Argentina*
[c] *Laboratorio de Servicios a la Industria y al Sistema Científico (UNLP-CIC-CONICET) Gonnet, Buenos Aires, Argentina*

Received 4 December 2006; received in revised form 26 March 2007; accepted 26 March 2007
Available online 3 April 2007

Abstract

Two new phosphoramidates with formula $C_6H_5OP(O)(NHC_6H_{11})_2$ (**1**) and $[N(CH_3)(C_6H_{11})]P(O)(2\text{-}C_5H_4N\text{-}NH)_2$ (**2**) were synthesized and characterized by ^1H, ^{13}C, ^{31}P NMR and IR spectroscopies and elemental analyses. The crystal structures of these compounds were determined using X-ray crystallography. Compound **1** [triclinic, $P\bar{1}$, $a = 8.8679(16)$ Å, $b = 10.230(2)$ Å, $c = 12.511(2)$ Å, $\alpha = 95.918(4)°$, $\beta = 103.948(4)°$, $\gamma = 110.818(4)°$, $Z = 2$] forms a centrosymmetric dimmer via two equal intermolecular $P{=}O\cdots H{-}N$ hydrogen bonds. In this structure, intermolecular hydrogen bonds are also formed between the crystallization solvent and phosphoramidate molecules. Compound **2** [monoclinic, $P2_1/c$, $a = 11.4760(7)$ Å, $b = 18.5607(12)$ Å, $c = 8.6227(6)$ Å, $\beta = 108.751(5)°$, $Z = 4$] produces a one-dimensional polymeric chain through intermolecular $P{=}O\cdots H{-}N$ hydrogen bonds, and a weaker intramolecular $N\cdots H{-}N$ hydrogen bond has been also observed in the crystal. *Ab initio* quantum chemical calculations were performed for molecules **1** and **2** by the density functional three-parameter hybrid (DFT/B3LYP) and the Hartree–Fock (HF) methods, using the 6-31G* basis set. The compound **1**:CH_3OH pair was also calculated as observed in the crystal. The computed geometrical parameters are in good agreement with the experimental results.

Keywords: Phosphoramide compounds; NMR spectroscopy; X-ray crystallography; *Ab initio* quantum chemical calculations

---

1. Introduction

Compounds with phosphorus-containing structures are an important part of chemistry, because of their applications in medicine [1,2], fertilizers, pesticides and plant growth regulators [3]. Recently, research on phosphoramides attracted attention due to their different applications in agriculture [4] and biochemistry [5]. Many authors have considered the substituent effects on the NMR and IR spectra of phosphoramidicacid esters [6,7], and various theories about the steric and electronic effects on phosphorus chemical shifts in phosphoryl compounds have been reviewed [8]. The synthesis, structures and complexation of some phosphoramides have been also reported [9,10]. Furthermore, *ab initio* studies were performed on different molecular derivatives of phosphine oxide and sulfide [11,12], polyphosphorus acid anhydrides [13], phosphates [14], phosphinates [15] and phosphonates [16–19]. The first evidence for a catalytic bridging in the active site of phosphodiesterase was obtained by computational methods [20]. Herein, we have investigated the synthesis,

---

[*] Corresponding authors. Tel.: +98 021 88011001x4422; fax: +98 021 88009730.
E-mail addresses: gholi_kh@modares.ac.ir (K. Gholivand), carlosdv@quimica.unlp.edu.ar (C.O. Della Védova).

0022-2860/$ - see front matter © 2007 Elsevier B.V. All rights reserved.
doi:10.1016/j.molstruc.2007.03.047

spectroscopic characterization, X-ray crystal structures and *ab initio* quantum chemical calculations of two new phosphoramides with formula $C_6H_5OP(O)(NHC_6H_{11})_2$ (**1**) and $[N(CH_3)(C_6H_{11})]P(O)(2\text{-}C_5H_4N\text{-}NH)_2$ (**2**). The experimental data were supplemented by using *ab initio* (HF) and DFT (B3LYP) quantum chemical calculations.

2. Experimental

2.1. Spectroscopic measurements

^{1}H, ^{13}C and ^{31}P NMR spectra were recorded on a Bruker Avance DRS 500 spectrometer. ^{1}H and ^{13}C chemical shifts were determined relative to internal TMS, ^{31}P chemical shifts relative to 85% H_3PO_4 as external standard. Infrared (IR) spectra of solid compounds in KBr pellets were recorded on a Shimadzu model IR-60 spectrometer. Elemental analyses were performed using a Heraeus CHN-O-RAPID apparatus. Melting points were obtained with an Electrothermal instrument. $C_6H_5OP(O)Cl_2$ [21] and $[N(CH_3)(C_6H_{11})]P(O)Cl_2$ [22] were synthesized according to the literature method.

2.2. X-ray measurements

X-ray data of compounds **1** and **2** were collected on a Bruker SMART 1000 CCD single crystal diffractometer with graphite monochromated MoKα radiation ($\lambda = 0.71073$ Å). The structures were refined with SHELXL-97 [23] by full matrix least squares on F^2. The positions of hydrogen atoms were obtained from the difference Fourier map. Routine Lorentz and polarization corrections were applied and an absorption correction was performed using the SADABS program for compound **2** [24].

2.3. Computational details

Full geometry optimizations were performed for isolated molecules **1** and **2** as well as for a compound **1**:CH_3OH pair, as observed in the crystal. Optimized structures were calculated by the density functional three-parameter hybrid (DFT/B3LYP) and the Hartree–Fock (HF) methods, using the 6-31G* basis set. Subsequently, the harmonic frequencies were calculated at the same level of approximation with the Gaussian98 program [25]. No scale factor was used in the calculated frequencies.

2.4. Syntheses

2.4.1. N,N′-bis(cyclohexyl)-phenyl phosphoramidicacid ester (1)

To a stirred solution of phenyl dichlorophosphate (1.05 g, 5 mmol) in dry acetonitrile (35 ml), a solution of cyclohexylamine (1.98 g, 20 mmol) was added dropwise at −5 °C. After 12 h, the solvent was evaporated under vacuum and the oily product was washed with distilled water and recrystallized from a mixture of CH_3OH/H_2O. Yield: 78%. m.p. 118 °C. Anal. Calc. for $C_{18}H_{29}N_2O_2P$: C 64.26, H 8.68, N 8.33. Found: C 64.24, H 8.67, N 8.32%. ^{31}P NMR (d_6-DMSO): 10.81 (m). ^{13}C NMR (d_6-DMSO): 24.96 (s), 25.16 (s), 35.11 (d, $^3J(P,C) = 5.0$ Hz, CH_2), 35.22 (d, $^3J(P,C) = 5.0$ Hz, CH_2), 50.01 (s), 120.30 (d, $^3J(P,C) = 4.9$ Hz, C_{ortho}), 123.18 (s), 129.10 (s), 151.93 (d, $^2J(P,C) = 6.4$ Hz, C_{ipso}). ^{1}H NMR (d_6-DMSO): 1.00–1.17 (m, 10H), 1.47–1.75 (m, 12H), 2.86 (m, 2H), 4.49 (dd, $^2J(P,H) = 10.2$ Hz, $^3J(H,H) = 9.5$ Hz, 2H, NH), 7.05 (t, $^3J(H,H) = 7.6$ Hz, 1H, Ar-H), 7.15 (d, $^3J(H,H) = 7.6$ Hz, 2H, Ar-H), 7.28 (t, $^3J(H,H) = 7.6$ Hz, 2H, Ar-H). IR (KBr, cm^{-1}): 3230 (m), 2920 (s), 1585 (m), 1484 (s), 1439 (s), 1222 (m), 1199 (s, νP=O), 1166 (w), 1099 (s), 1021 (m), 938 (m), 910 (s), 747 (s), 610 (w), 580 (m).

2.4.2. N-methylcyclohexyl-N′,N″-bis(2-pyridinyl) phosphoric triamide (2)

To a stirred solution of *N*-methylcyclohexyl phosphoramide dichloride (2.31 g, 10 mmol) in dry acetonitrile (30 ml), a solution of 2-aminopyridine (3.76 g, 40 mmol) was added dropwise at −5 °C. After 15 h, the solvent was evaporated under vacuum and the oily product was washed with distilled water and recrystallized from a mixture of CH_3OH/H_2O. Yield: 73%. m.p. 225 °C. Anal. Calc. for $C_{17}H_{24}N_5OP$: C, 59.12; H, 7.00; N, 20.28. Found: C, 59.10; H, 7.01; N, 20.27%. ^{31}P NMR (d_6-DMSO): 3.66 (m). ^{13}C NMR (d_6-DMSO): 25.03 (s), 25.57 (s), 27.52 (d, $^2J(P,C) = 5.4$ Hz, *N*-CH_3), 30.02 (d, $^3J(P,C) = 2.4$ Hz, CH_2), 54.11 (s), 111.18 (d, $^3J(P,C) = 4.1$ Hz, C_{ortho}), 116.13 (s), 137.62 (s), 147.75 (s), 154.62 (d, $^2J(P,C) = 4.1$ Hz, C_{ipso}). ^{1}H NMR (d_6-DMSO): 0.92–1.63 (m, 11H), 2.53 (d, $^3J(P,H) = 10.7$ Hz, 3 H, *N*-CH_3), 6.84 (t, $^3J(H,H) = 6.7$ Hz, 2H, Ar-H), 7.01 (d, $^3J(H,H) = 6.7$ Hz, 2H, Ar-H), 7.60 (t, $^3J(H,H) = 6.7$ Hz, 2H, Ar-H), 8.07 (d, $^2J(PNH) = 8.6$ Hz, 2H, NH), 8.13 (d, $^3J(H,H) = 6.7$ Hz, 2H, Ar-H). IR (KBr, cm^{-1}): 3390 (m), 3145 (s), 2925 (s), 1588 (s), 1456 (s), 1394 (s), 1301 (s), 1264 (m), 1193 (s, νP=O), 1140 (s), 1006 (s), 978 (s), 924 (s), 810 (w), 770 (s), 640 (w), 540 (m), 499 (s).

3. Results and discussion

In this study, we prepared two new phosphoramidates from the reaction of phenyl dichlorophosphate and *N*-methylcyclohexyl phosphoramide dichloride intermediate with the corresponding amines, respectively (Scheme 1). Some characteristic spectroscopic data of these compounds are given in Table 1. ^{1}H NMR spectra of compounds **1** and **2** indicate $^2J(P,H)$ coupling constants of 10.2 and 8.6 Hz, respectively. $^3J(P,H)$ coupling constant (10.7 Hz) is observed for the splitting of *N*-CH_3 protons with phosphorus atom in **2**, which is in agreement with our previously reported values for related molecules [22]. ^{13}C NMR spectrum of molecule **1** shows five signals for aliphatic cyclohexyl groups. Two of them are doublet peaks with two equal $^3J(P,C) = 5.0$ Hz. Therefore, the two CH_2 carbon atoms separated by three bond distances from phosphorus

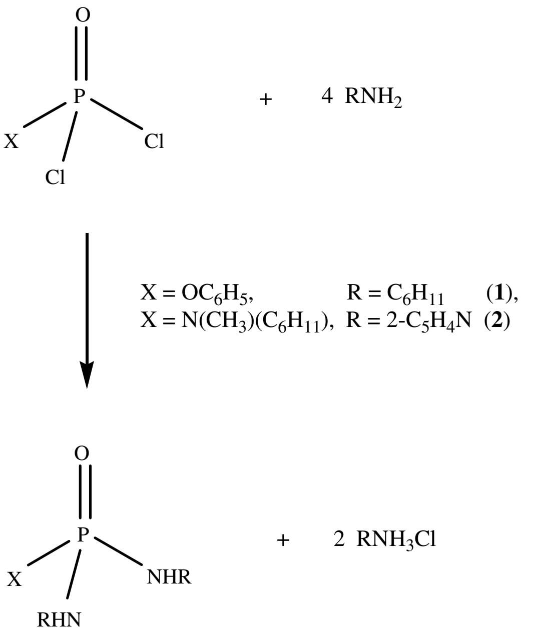

Scheme 1. Preparation pathway of compounds **1** and **2**.

atom are not equivalent each other. The ^{13}C NMR spectrum of **2** shows five signals for *N*-methylcyclohexyl moiety with $^{2}J(\mathrm{P,C}) = 5.4$ Hz (for *N*-methyl group) and $^{3}J(\mathrm{P,C}) = 2.4$ Hz (for CH_2 group). Also, $^{2,3}J(\mathrm{P,C})$ coupling constants for aromatic carbon atoms was obtained in these molecules. The $J(\mathrm{P,C})$ coupling constant observed for compound **1** are as follow: $^{2}J(\mathrm{P,C}) = 6.4\ \mathrm{Hz} > {}^{3}J(\mathrm{P,C}) = 4.9$ Hz, whereas in compound **2**, $^{2}J(\mathrm{P,C}) = {}^{3}J(\mathrm{P,C}) = 4.1$ Hz.

Single crystals of compounds **1** and **2** were obtained from CH_3OH/H_2O solutions at room temperature. The crystallographic data and the details of the X-ray analysis are represented in Table 2, selected bond lengths and angles for compounds **1** and **2** are given in Tables 3 and 4, respectively. Hydrogen bonding data of these structures are presented in Table 5. Molecular structures are shown in Figs. 1 and 2, and unit cell packing in Figs. 3 and 4, for compounds **1** and **2**, respectively.

Compound **1** forms a centrosymmetric dimmer via two equivalent intermolecular P(1)—O(1)···H(2N)—N(2) hydrogen bonds. Also, the O(1) and N(1) atoms of compound **1** form intermolecular O(1)···H(1O)—O(1S) and O(1S)···H(1N)—N(1) hydrogen bonds with solvent molecule. Therefore, each dimmer is connected to four molecules of CH_3OH. Linking of these hydrogen bonds leads to a one-dimensional polymeric chain in the crystalline lattice. Here, the *d*(H···A) distances for the hydrogen bonding between solvent and phosphoramide molecule are shorter (1.90 and 1.86 Å) than that of intermolecular —P=O···H—N hydrogen bond (2.03 Å), probably due to the strong interaction of small solvent molecule with compound **1**, than that between two phosphoramidates molecules. Cameron et al. have been reported that the co-crystallization of donor solvents (or arylammonium chloride) in aryl derivatives precludes extended hydrogen bonding networks [26]. On the other hand, compound **2** produces a one-dimensional polymeric chain from intermolecular P(1)—O(1)···H(1N)—N(1) hydrogen bonds (with *d*(H···A) = 1.96 Å) and also a weaker intramolecular N(2)···H(3N)—N(3) hydrogen bond (*d*(H···A) = 2.67 Å).

The P=O bond lengths in molecules **1** and **2** are 1.4877(15) and 1.4793(12) Å, respectively, that are larger than the normal P=O bond length (1.45 Å for $P(O)Cl_3$) [3]. In compound **2**, the $\mathrm{P{-}N_{aromatic}}$ bond lengths are longer than the $\mathrm{P{-}N_{aliphatic}}$ bond length because of the interaction of $\mathrm{N_{aromatic}}$ with π resonance system of 2-pyridinyl ring results in a shorter $\mathrm{C{-}N_{aromatic}}$ bond length (the $\mathrm{C{-}N_{aromatic}}$ bond lengths are shorter than the $\mathrm{C{-}N_{aliphatic}}$ bond lengths). All of these P—N bonds are shorter than the typical P—N single bond length (1.77 Å for $NaHPO_3NH_2$ [3]). The nitrogen environments in the amidic groups are nearly planar. In effect, for compound **1**, the angles C(7)—N(1)—P(1), P(1)—N(1)—H(1N) and C(7)—N(1)—H(1N) have values of 125.2(2)°, 112.6(2)° and 118.4(2)°, respectively with average 118.7°. Similarly, the sum of surrounding angles around N(2) atom is 358.3°. Similar results were obtained for the nitrogen atoms of structure **2**, which indicate sp^2 hybridization for the nitrogen atoms (deviation from the ideal value, 120°, may be caused by electronic and/or steric effects).

The conformational space around the central phosphoric group of the molecule **1** has been studied using the B3LYP/6-31G* level of theory. The molecular structure determined in the X-ray diffraction study was used as the initial structure for single point calculations for fixed values of the O=P—N(2)—H(2N), O=P—N(1)—H(1N) and O=P—O(2)—C(1) dihedral angles. For this purpose, the SCAN option was used as implemented in the Gaussian program [25], by varying each dihedral angle from 0° to 180°, in step of 30°. According to these calculations, the most stable conformation is similar to the structure found in the crystal. Chair and planar carbon skeleton were calculated for the cyclohexyl and phenyl rings, respectively. Slight conformational differences, which are mainly reflected in the values observed for dihedral angle around

Table 1
Selected NMR spectroscopic data for compounds **1** and **2**

Compound	$\delta(^{31}\mathrm{P})$ (ppm)	$\delta(\mathrm{N{-}^{1}H})$ (ppm)	$\delta(^{13}\mathrm{CH_2})$ (ppm)	$^{2}J(\mathrm{PH})$ (Hz)	$^{3}J(\mathrm{PH})$ (Hz)	$^{3}J(\mathrm{P,C_{aliphatic}})$ (Hz)	$^{2}J(\mathrm{PC_{aromatic}})$ (Hz)	$^{3}J(\mathrm{PC_{aromatic}})$ (Hz)
1	10.81	4.49(dd)	35.11(d), 35.22(d)	10.2	–	5.0, 5.0	6.4	4.9
2	3.66	8.07(d)	30.02(d)	8.6	10.7	2.4, 5.4	4.1	4.1

Table 2
Crystallographic data for compounds **1** and **2**

	1	**2**
Empirical formula	$C_{19}H_{33}N_2O_3P$	$C_{17}H_{24}N_5OP$
Formula weight	368.44	345.38
Temperature (K)	120(2)	120(2)
Wavelength (Å)	0.71073	0.71073
Crystal system, space group	Triclinic, $P\bar{1}$	Monoclinic, $P2_1/c$
Unit cell dimensions		
a (Å)	8.8679(16)	11.4760(7)
b (Å)	10.230(2)	18.5607(12)
c (Å)	12.511(2)	8.6227(6)
α (°)	95.918(4)	90.0
β (°)	103.948(4)	108.751(5)
γ (°)	110.818(4)	90.0
V (Å^3)	1007.1(3)	1739.2(2)
Z, calculated density (Mg m^{-3})	2, 1.215	4, 1.319
Absorption coefficient (mm^{-1})	0.156	0.173
F(000)	400	736
Crystal size (mm)	$0.25 \times 0.20 \times 0.05$	$0.20 \times 0.20 \times 0.15$
θ range for data collection (°)	2.18–28.09	1.87–30.01
Limiting indices	$-11 \leqslant h \leqslant 10$; $-13 \leqslant k \leqslant 12$; $-16 \leqslant l \leqslant 15$	$-16 \leqslant h \leqslant 15$; $-26 \leqslant k \leqslant 25$; $-12 \leqslant l \leqslant 12$
Reflections collected/unique [R(int)]	7594/4829 [0.0345]	20044/5034 [0.0552]
Completeness to θ (%)	98.2	99.3
Absorption correction	None	Semi-empirical from equivalents
Max. and min. transmission	–	0.9786 and 0.9633
Refinement method	Full-matrix least-squares on F^2	Full-matrix least-squares on F^2
Data/restraints/parameters	4829/0/227	5034/0/218
Goodness-of-fit on F^2	0.837	1.065
Final R indices	$R_1 = 0.0489$, $wR_2 = 0.0921$	$R_1 = 0.0496$, $wR_2 = 0.0877$
R indices (all data)	$R_1 = 0.1038$, $wR_2 = 0.1069$	$R_1 = 0.0872$, $wR_2 = 0.0945$
Largest diff. peak and hole (e Å^{-3})	0.313 and −0.279	0.397 and −0.449

the P—N(2) and P—O(2) single bonds, are probably caused by intermolecular interactions in the crystal. It is well known that intermolecular interactions may cause the molecular geometry in the solid phase to be different from that of the free molecule.

Full geometry optimizations of isolated molecules were performed, also for a pair of compound **1**:CH_3OH molecules interacting through N(1)—H⋯O(methanol) hydrogen bond. This model represents the fragment of a chain in the crystal formed by molecules of compound **1** linked by hydrogen bond assisted by co-crystallization of solvent molecules. Calculations have predicted the N(1)—H(1N)⋯O(1S) hydrogen bond length of about 2.01 Å, and the N(1)—H(IN)⋯O(1S) bond angle of 159°, the N(1)⋯O(1S) distance being 2.99 Å. The experimentally determined N(1)⋯O(1S) length is similar, 2.84 Å, however, the N(1)—H(IN)⋯O(1S) bond angle of 163.8° shows less deviation from linearity than the calculated structure.

Table 3 compares calculated selected geometric parameters with the experimental data. As follows from this comparison, the bond lengths and angles calculated for the central phosphoric moiety show quite good agreement with experiment. The geometric parameters of the diamide phosphoric $(—NH)_2P{=}O$ groups are expected to be sensitive to the formation of intermolecular hydrogen bonding in crystal. This is reflected mainly in the O=P—N bond angles, with values of 108.6° and 121.5° for O=P—N(1) and O=P—N(2), respectively. These values are well reproduced by quantum chemical calculations, where; obviously, intermolecular hydrogen bonds are not present. Thus, the difference in this bond angle seems to be related with attractive intramolecular interactions between the N(2)—H amide group and the P=O double bond. The short non-bonded H(2N)⋯O(1) distance (2.629 Å) and the nearly *syn* orientation of the P=O and the N(2)—H bonds support this assumption [the O=P—N(2)H dihedral angle is −28.1° in the crystal].

Calculations have revealed that the N(1)—H bond involved in intermolecular hydrogen bonding is longer (by 0.012 Å) than the N(2)—H bond. Thus, the two amine groups for the compound **1** in the solid phase become nonequivalent. In such a case, the presence of two bands are expected in the characteristic amide stretching region, which correspond to two different ν(N—H) stretching vibrations.

Table 6 gathers selected experimental and calculated frequencies for compound **1**. The simulated infrared spectrum for the molecule **1** is given in Fig. 5. Two intense bands appear in the IR spectrum at 1222 and 910 cm^{-1} and are assigned to the ν(O—C) and ν(O—P) stretching modes of the phenoxyphosphorus moiety, respectively. These normal modes are calculated at 1254 and 908 cm^{-1}, respectively. The calculated P=O stretching vibration [ν(P=O)] is predicted as an intense band at 1239 cm^{-1}, which correlates

Table 3
Selected experimental (X-ray) and calculated geometrical parameters for compound **1** (bond lengths in Å, bond angles in °)[a]

Parameter	X-ray	HF/6-31G*	B3LYP/6-31G*	B3LYP/6-31G*[b]
P(1)—O(1)	1.4877(15)	1.460	1.490	1.489
P(1)—O(2)	1.6021(15)	1.610	1.650	1.671
P(1)—N(1)	1.6160(16)	1.650	1.670	1.662
P(1)—N(2)	1.6160(17)	1.630	1.660	1.654
O(2)—C(1)	1.385(2)	1.370	1.380	1.389
N(1)—C(7)	1.472(2)	1.460	1.470	1.471
N(2)—C(13)	1.470(3)	1.450	1.460	1.459
N(1)—H(1N)	0.967	0.991	1.010	1.003
N(1)—H(2N)	0.926	0.990	1.010	0.990
C(1)—C(2)	1.379(3)	1.380	1.398	1.385
C(1)—C(6)	1.385(3)	1.380	1.398	1.385
C(2)—C(3)	1.387(3)	1.380	1.398	1.385
O(1)—P(1)—N(1)	121.55(9)	119.6	121.2	122.0
O(1)—P(1)—N(2)	108.62(9)	109.7	110.3	110.1
O(1)—P(1)—O(2)	110.72(8)	114.7	115.1	113.6
N(1)—P(1)—N(2)	106.84(9)	106.8	104.5	105.6
N(1)—P(1)—O(2)	96.26(8)	95.7	94.9	95.3
N(2)—P(1)—O(2)	112.43(9)	109.2	110.0	109.0
P(1)—O(2)—C(1)	127.24(14)	126.6	125.4	122.7
P(1)—N(1)—C(7)	125.24(15)	121.4	120.4	119.5
P(1)—N(2)—C(13)	127.25(15)	128.3	127.4	127.9
P(1)—N(2)—H(2N)	116.9	113.6	112.3	113.8
P(1)—N(1)—H(1N)	112.6	113.9	112.6	114.4
C(7)—N(1)—H(1N)	118.4	116.7	115.8	116.8
C(13)—N(2)—H(2N)	114.1	114.2	113.5	114.0
C(2)—C(1)—O(2)	124.1(2)	122.4	123.2	112.1
C(6)—C(1)—O(2)	115.59(19)	116.6	116.0	116.9
C(2)—C(1)—C(6)	120.28(15)	120.9	120.8	121.0
O(1)—P(1)—N(2)—H(N2)	−28.1	−11.0	−17.3	−15.6
O(1)—P(1)—N(1)—H(1N)	87.7	94.9	88.3	91.9
O(1)—P(1)—O—C(1)	43.8	50.4	45.6	52.7

[a] For atom numbering, see Fig. 1.

[b] Calculated parameters for the compound **1**:CH_3OH pair.

well with the observed band at 1199 cm^{-1} in the IR spectrum of solid (**1**), and with reported data for similar substituted phosphate species [22]. The characteristic phosphoramidate ν(P—N) stretching modes are predicted at 1008 cm^{-1} [ν(P—N1)] and 1026 cm^{-1} [ν(P—N2)], frequency values that are in good agreement with the band observed at 1021 cm^{-1} in the IR spectrum. The ν(N—C) stretching modes for the amide groups are predicted as strong intensity bands, which differ slightly in their wavenumbers [1115 and 1126 cm^{-1} for the ν(N1—C7) and ν(N2—C13) modes, respectively]. In the experimental spectrum this region is dominated by a strong absorption cantered at 1099 cm^{-1}. The amide deformation modes are assigned to the bands at 1484 and 1439 cm^{-1} in the IR spectrum of solid (**1**), taking into account calculated values at 1471 and 1462 cm^{-1} for the δ(N2—H) and δ(N1—H), respectively. It is well known that the δ(N—H) overtone is generally observed in the IR spectra of amidates, because its intensity could be reinforced by the Fermi resonance effect with the N—H fundamental stretching mode [27]. For compound (**1**), the strong band at 2920 cm^{-1} was assigned to this overtone mode. In both experimental and simulated spectra, complicated pattern of absorptions were observed in the regions between 1200–1650 and 3000–3250 cm^{-1}, which originate from the diverse C—H stretching and deformation modes, respectively. Frequency calculations were done also for the molecule **1**:CH_3OH aggregate. Main differences are reflected in the ν(N1—H) stretching mode. In effect, while slight changes are calculated for the ν(N2—H) band location (7 cm^{-1}), an important red shift (135 cm^{-1}) is predicted for the ν(N1—H), together with an important enhancement in the band intensity with respect to the isolated molecule. These are the expected behavior for stretching modes which are directly involved in hydrogen bond interactions [28]. The high frequency region of the IR spectrum of solid (**1**) shows the presence of a band with medium intensity at 3230 cm^{-1}, which could be related with the ν(N—H) mode for the interacting N1—H amidate moiety.

Selected optimized geometrical parameters for compound (**2**) are listed in Table 6 and compared with the X-ray experimental data. The global conformation of the molecule **2** seems to be similar in both the solid and gaseous phases, since quite similar values are observed when experimental and calculated dihedral angles are compared. Chair and planar skeleton were calculated for the

Table 4
Selected experimental (X-ray) and calculated geometrical parameters for compound **2** (bond lengths in Å, bond angles in °)[a]

	X-ray	HF/6-31G*	B3LYP/6-31G*
P(1)—O(1)	1.4793(12)	1.460	1.489
P(1)—N(5)	1.6386(15)	1.653	1.670
P(1)—N(1)	1.6587(15)	1.694	1.730
P(1)—N(3)	1.6617(15)	1.665	1.680
N(3)—C(6)	1.396(2)	1.471	1.400
N(1)—C(1)	1.397(2)	1.457	1.390
N(2)—C(1)	1.332(2)	1.323	1.331
N(2)—C(2)	1.350(2)	1.375	1.340
N(3)—C(6)	1.396(2)	1.400	1.391
N(4)—C(6)	1.342(2)	1.324	1.330
N(4)—C(7)	1.349(2)	1.393	1.341
N(5)—C(11)	1.465(2)	1.471	1.460
N(5)—(C12)	1.485(2)	1.471	1.480
N(2)···N(3)	2.995	2.973	2.830
O(1)—P(1)—N(1)	115.13(8)	116.5	115.7
O(1)—P(1)—N(3)	114.71(7)	116.6	118.7
O(1)—P(1)—N(5)	111.45(7)	111.7	111.7
N(5)—P(1)—N(1)	107.29(8)	106.4	106.5
N(5)—P(1)—N(3)	105.65(8)	102.	103.1
N(1)—P(1)—N(3)	101.70(8)	99.6	99.4
P(1)—N(5)—C(11)	119.44(12)	120.1	119.7
P(1)—N(5)—C(12)	119.69(12)	121.0	119.4
C(11)—N(5)—C(12)	117.31(14)	118.5	118.6
P(1)—N(1)—C(1)	125.66(13)	128.0	129.4
P(1)—N(3)—C(6)	129.23(13)	127.8	126.8
C(1)—N(2)—C(2)	116.76(16)	118.6	118.5
C(1)—N(1)—H(N1)	114.6	112.9	113.4
P(1)—N(1)—H(1N)	119.6	115.2	113.4
C(1)—N(2)—C(2)	116.76(16)	119.0	118.4
C(6)—N(4)—C(7)	117.1(2)	118.5	117.9
O(1)—P(1)—N(5)—C(11)	171.9	170.1	179.9
O(1)—P(1)—N(5)—C(12)	230.0	4.5	17.5
O(1)—P(1)—N(1)—C(1)	61.4	64.2	75.7
O(1)—P(1)—N(3)—C(6)	49.7	48.8.	50.6
P(1)—N(1)—C(1)—N(2)	7.5	37.0	32.8
P(1)—N(3)—C(6)—N(4)	−171.4	−179.5	−161.3

[a] For atom numbering, see Fig. 3.

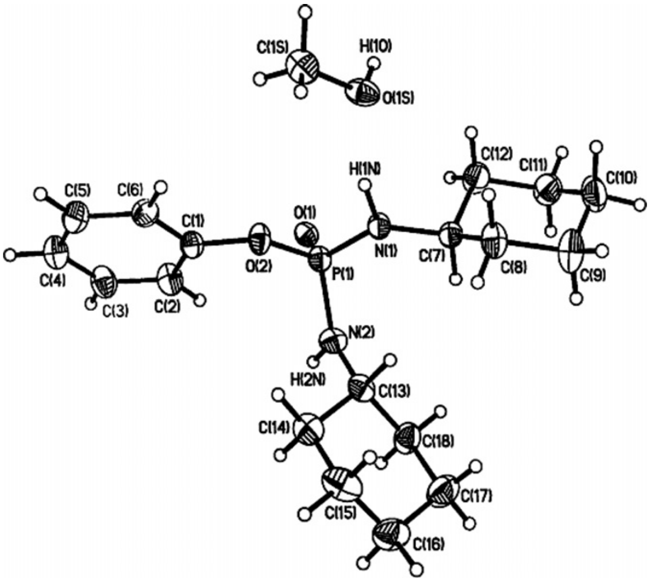

Fig. 1. Ortep view of compound **1**, $C_6H_5OP(O)(NHC_6H_{11})_2$, with 50% probability ellipsoids.

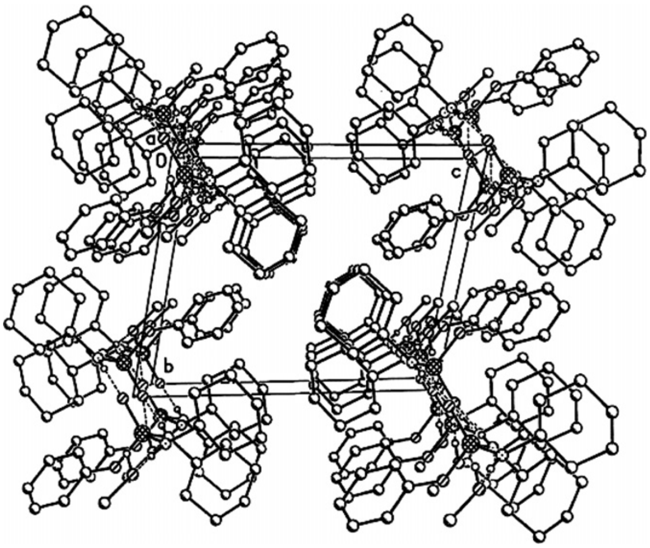

Fig. 2. Unit cell packing of compound **1**, $C_6H_5OP(O)(NHC_6H_{11})_2$, along *a* axis.

cyclohexyl and 2-pyridinyl rings, respectively. Similar geometric parameters are obtained by both HF and B3LYP applied methods. These results are in agreement with the experimental values obtained from the X-ray analysis, again taking into account that theoretical calculations were performed for the molecule isolated in vacuum. Differences in the bond lengths and in bond angles are smaller than ca. 0.07 Å and 4°, respectively. The considerable differences between the calculated and experimental data of the bond lengths corresponds to the P—N(5) bond in both HF and DFT methods. The largest differences between experimental and calculated angle values are 4.0° and 3.8° for O=P—N(3) and P—N(3)—C(6) in B3LYP/6-31G* method.

Table 5
Hydrogen bonds for compounds **1** and **2** (distances in Å and angles in °)

Compound	*d*(H···A)	*d*(D—H)	*d*(H···A)	∠DHA	*d*(D···A)
1	N(1)—H(1N)···O(1S)	0.97	1.90	164.0	2.843(3)
	O(1S)—H(1O)···O(1) [$-x+1, -y, -z$]	0.87	1.86	169.0	2.721(2)
	N(2)—H(2N)···O(1) [$-x, -y, -z$]	0.93	2.03	170.0	2.943(2)
2	N(1)—H(1N)···O(1) [$x, -y+1/2, z-1/2$]	0.94	1.96	164.0	2.871(2)
	N(3)—H(3N)···N(2)	0.92	2.67	101.6	2.995(2)

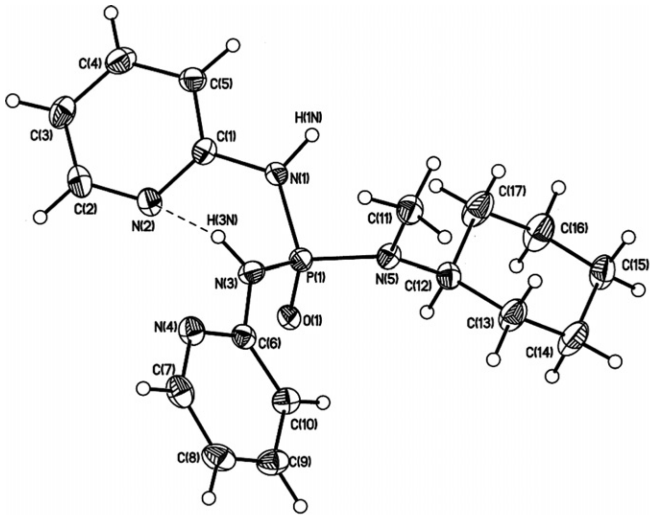

Fig. 3. Ortep view of compound **2**, $[N(CH_3)(C_6H_{11})]P(O)(2-C_5H_4N-NH)_2$, with 50% probability ellipsoids.

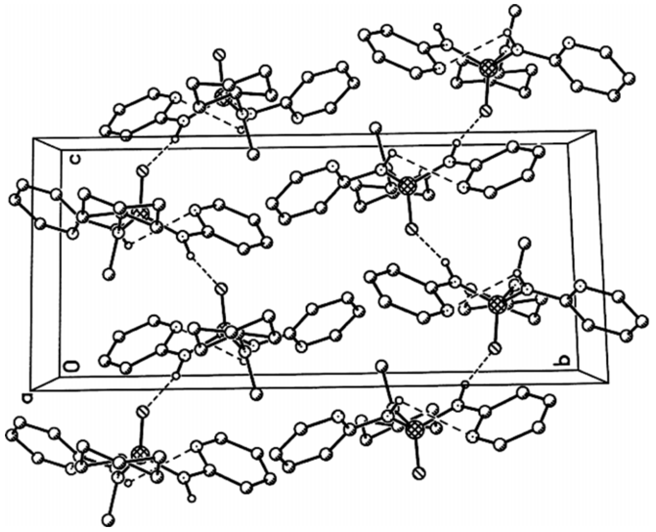

Fig. 4. Unit cell packing of compound **2**, $[N(CH_3)(C_6H_{11})]P(O)(2-C_5H_4N-NH)_2$.

Table 6
Selected experimental (KBr pellets) and calculated (B3LYP/6-31G*) frequencies (cm^{-1}) for compounds **1** and **2**

Mode	Compound **1**		Compound **2**	
	Experimental	Calculated	Experimental	Calculated
ν(N—H)[a]	3230	3578 ν(N2—H)	3390	3575 ν(N1—H)
		3548 ν(N1—H)	3145	3368 ν(N3—H)
δ(N—H)[b]	1484	1471 δ(N2—H)	1588	1499
	1439	1462 δ(N1—H)	1456	1495
			1394	1458
			1301	1431
ν(P=O)	1199	1239	1193	1269
ν(O—C)	1222	1254		
ν(O—P)	910	908		
ν(N—C)[b]	1099	1115 ν(N1—C7) 1126 ν(N2—C13)		
ν(P—N)	1021	1026 ν(P—N2)	978	985 ν(P—N5)
		1008 ν(P—N1)	924	949 ν(P—N3)
			810	890 ν(P—N1)

[a] For the compound (**1**):CH_3OH pair, calculated ν(N2—H) and ν(N1—H) values are 3585 and 3413 cm^{-1}, respectively.

[b] δ(N—H) and ν(N—C) normal modes are strongly coupled in compound (**2**), see text.

Analogous differences for the HF/6-31G* calculations are 1.9° and 2.4°, respectively.

The intramolecular hydrogen bond interaction between one amide group and a nitrogen atom in the 2-pyridinyl ring [N(3)—H···N(2)] is well reproduced by quantum chemical calculations. The calculated values for the O=P—NC dihedral angles are very close to the experimental ones, and the experimentally found N(2)···N(3) nonbonded distance (2.995 Å) accords well with the calculated values (2.973 and 2.830 Å for the HF and B3LYP methods, respectively).

Table 6 gathers selected experimental and calculated frequencies for compound **2**, while the simulated infrared spectrum is given in Fig. 6. A group of four bands with high intensities, which appear at 1499, 1495 and 1458, 1431 cm^{-1} are assigned as coupled modes of vibrations between the two ν(N—C) stretching modes and the two δ(N—H) amide deformation modes. These modes are observed in the IR spectra of solid (**2**) as four absorption bands with strong intensity, which are observed at 1588, 1456, 1394 and 1301 cm^{-1}. As in the previous case, a strong absorption at 2925 cm^{-1} can be assigned to the overtone associated with the δ(N—H) amide deformation mode. The characteristic P=O stretching vibration is predicted as a band of medium intensity located at 1269 cm^{-1}, which correlated very well with the experimental value at 1193 cm^{-1}. The ν(P—N) stretching modes appear at 978, 924 and 810 cm^{-1} in the IR spectrum, which were assigned as ν(P—N5), ν(P—N3) and ν(P—N1), respectively (see Table 6). As in the previous spectrum, the complicated pattern of absorption in the regions of 1200–1650 and 3000–3250 cm^{-1} originates from the diverse C—H stretching and deformation modes, respectively. It is worthy to note the feature observed in the high-wavenumber region of the calculated spectrum. The highest normal mode of vibration corresponds to the ν(N1—H) stretching, which is calculated at 3575 cm^{-1} and posses a weak intensity. On the other hand, ν(N3—H) normal mode is assigned to the very intense absorption located at 3368 cm^{-1}, reflecting the occurrence of N(2)···H—N(3) intramolecular hydrogen bond interaction [27]. These modes appear at 3390 and

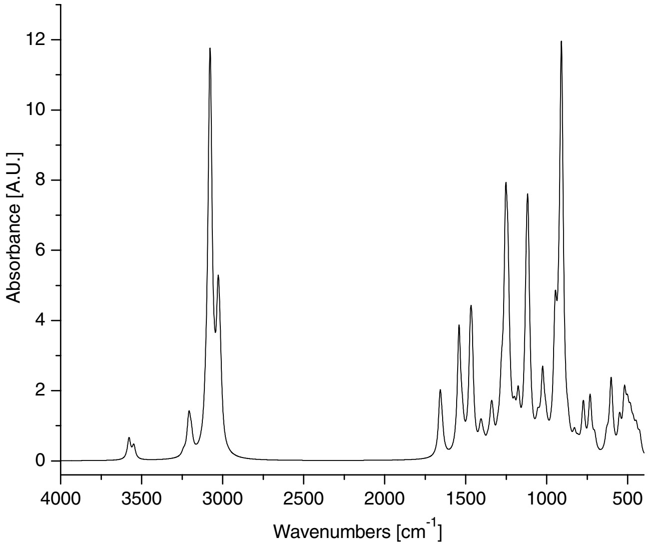

Fig. 5. Simulated infrared spectrum for compound **1** from B3LYP/6-31G* calculation.

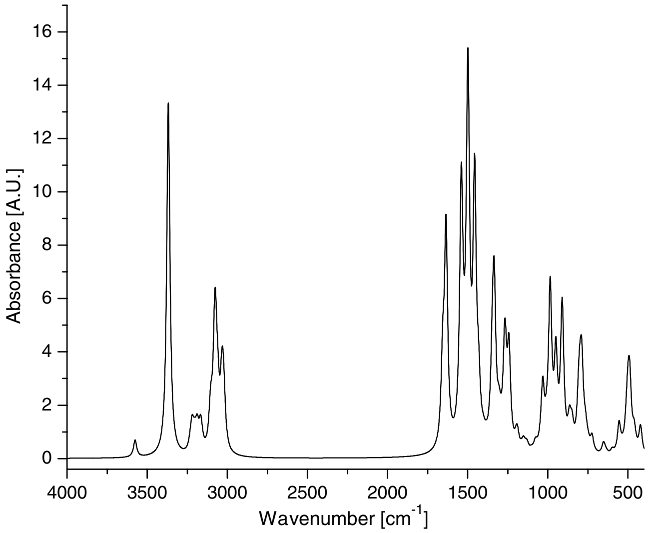

Fig. 6. Simulated infrared spectrum for compound **2** from B3LYP/6-31G* calculation.

3145 cm^{-1} in the IR spectrum of solid (**2**) as a medium and strong absorption, respectively.

4. Conclusions

Two new phosphoramidates were synthesized and characterized by multinuclear NMR, IR spectroscopy and elemental analyses. The crystal structures of these compounds were determined using X-ray crystallography. Compound **1** forms a centrosymmetric dimmer via two equal intermolecular P═O···H—N hydrogen bonds. Compound **2** crystallizes forming a one-dimensional polymeric chain through intermolecular P═O···H—N hydrogen bonds, while weaker intramolecular N···H—N hydrogen bond has been also observed.

^{31}P NMR spectra show that δ(^{31}P) in compound **1** occurs at down field relative to that of **2**. IR spectra revealed that the ν(P═O) stretching mode for compound **1** appears at 1199 cm^{-1}, while for compound **2** this mode is assigned to a strong intensity band at 1193 cm^{-1}. These observations indicate that the substituents at the phosphorus atom in compound **1** are more electron withdrawing than in compound **2** resulting in a more deshielded P atom and a stronger P═O bond. A noticeable contradiction in the trend of both frequencies of the P═O stretching normal mode of vibration for **1** and **2** and corresponding bond distances results apparent. Thus, whereas the experimental frequencies for **1** and **2** are 1199 and 1193 cm^{-1} the corresponding bond distances are 1.4877(15) and 1.4793(12) Å, respectively. A close analysis of these normal modes of vibration for **1** and **2** reveals a high degree of mixture being the normal coordinate not only based on the P═O but also on the O—C and N—C internal coordinates of the methoxyphenyl and the 2-pyridinyl rings for **1** and **2**, respectively.

5. Supplementary data

Crystallographic data for the structures **1** and **2** in this paper have been deposited with Cambridge Crystallographic Data Center as supplementary publication nos. CCDC 601411 ($C_{19}H_{33}N_2O_3P$) and CCDC 601410 ($C_{17}H_{24}N_5OP$). Copies of the data may be obtained, free of charge, on application to CCDC, 12 Union Road, Cambridge CB2 1EZ, UK (fax: +44 1223 336033; e-mail: deposit@ccdc.cam.ac.uk or http://www.ccdc.cam.ac.uk).

Acknowledgements

Financial support by the Research Council of Tarbiat Modarres University, Volkswagen-Stiftung and the Deutsche Forschungsgemeinschaft is gratefully acknowledged. The Argentinean authors thank the Consejo Nacional de Investigaciones Científicas y Técnicas (CONICET), the Comisión de Investigaciones Científicas de la Provincia de Buenos Aires (CIC), the Facultad de Ciencias Exactas, Universidad Nacional de La Plata, República Argentina for financial support. CODV especially acknowledges the DAAD for its generous sponsorship of the DAAD Regional Program of Chemistry of the Republic of Argentina (supporting Latin-American students for a PhD program in La Plata). The authors acknowledge Supercomputer Centre of the Secretary for the Technology, Science and Productive Innovation (SECyT), República Argentina, for computational time at the Clementina II computer.

References

[1] R. Hannuniemi, L. Lauren, H. Puolijoki, Drugs Today 27 (1991) 375.
[2] J.A. Kanis, E.V. McCloskey, Calcium Metab. Prog. Basic Clin. Pharmacol. 4 (1990) 89.

[3] D.E.C. Corbridge, Phosphorus, an Outline of its Chemistry, Biochemistry and Technology, Elsevier, The Netherlands, 1995.
[4] Y. Pang, T.M. Kollmeyer, F. Hong, J. Lee, P.I. Hammond, S.P. Haugabouk, S. Brimijoin, Biochem. Biol. 10 (2003) 491.
[5] A. Baldwin, Z. Huang, Y. Jounaidi, D.J. Waxman, Arch. Biochem. Biophys. 409 (2003) 197.
[6] F. Ibanenez, Spectrochim. Acta 38A (1982) 351.
[7] J.H. Letcher, J.R. Van Wazer, J. Chem. Phys. 44 (1966) 815.
[8] D.G. Gorenstein, Prog. Nucl. Magn. Reson. Spectrosc. 16 (1983) 1.
[9] (a) T. Chivers, M. Krahn, G. Schatte, M. Parvez, Inorg. Chem. 42 (2003) 3994;
(b) A. Armstrong, T. Chivers, M. Krahn, M. Parvez, G. Schatte, Chem. Commun. (2002) 2332.
[10] T. Chivers, M. Krahn, M. Parvez, G. Schatte, Chem. Commun. (2001) 1992.
[11] J.S. Kwiatkowski, J. Leszczynski, J. Phys. Chem. 96 (1992) 6636.
[12] Y. Akacem, O. Ouamerali, E. Kassab, E.M. Evleth, J. Phys. Chem. 96 (1992) 1697.
[13] C.S. Ewig, J.R. Van Wazer, J. Am. Chem. Soc. 110 (1988) 79.
[14] G. Lipari, C. Tosi, Theor. Chim. Acta 50 (1978) 169.
[15] M.S. Gordon, J.A. Boatz, M.W. Schmidt, J. Phys. Chem. 88 (1984) 2998.
[16] D.J. Pasto, J. Org. Chem. 50 (1985) 1014.
[17] J.R. Van Wazer, C.S. Ewig, J. Am. Chem. Soc. 108 (1986) 4354.
[18] J.P. Räsänen, M. Peräkylä, E. Pohjala, T.A. Pakkanen, J. Chem. Soc. Perkin Trans. 2 (1994) 1055.
[19] J.P. Räsänen, E. Pohjala, T.A. Pakkanen, J. Chem. Soc. Perkin Trans. 2 (1994) 2485.
[20] C.-G. Zhan, F. Zheng, J. Am. Chem. Soc. 123 (2001) 2835.
[21] H. Tolkimth, Ann. NY. Acad. Sci. 79 (Art 7) (1959) 189 (Dow Chem. Co., Midland, Mich.).
[22] K. Gholivand, S. Ghadimi, A. Forouzanfar, H. Naderimanesh, Magn. Reson. Chem. 39 (2001) 684.
[23] Sheldrick, G.M., 1998. SHELXTL v. 5.10, Structure Determination Software Suit, Bruker AXS, Madison, WI, USA.
[24] Sheldrick, G.M., 1998. In: SADABS v. 2.01, Bruker/Siemens Area Detector Absorption Correction Program, Bruker AXS, Madison, WI, USA.
[25] Frisch, M.J., Trucks, G.W., Schlegel, H.B., Scuseria, G.E., Robb, M.A., Cheeseman, J.R., Zakrzewski, V.G., Montgomery, J.A., Stratman, R.E., Burant, J.C., Dapprich, S., Millam, J.M., Daniels, A.D., Kudin, K.N., Strain, M.C., Farkas, O., Tomasi, J., Barone, V., Cossi, M., Cammi, R., Menucci, B., Pomelli, C., Adamo, C., Clifford, S., Ochterski, J., Petersson, G.A., Ayala, P.Y., Cui, Q., Morokuma, K., Malick, D.K., Rabuck, A.D., Raghavachari, K., Foresman, J.B., Cioslovski, J., Ortiz, J.V., Stefanov, B.B., Liu, G., Liashenko, A, Piskorz, P., Komaromi, I., Gomperts, R., Martin, R.L., Fox, D.J., Keith, T., Al-Laham, M.A., Peng, C.Y., Nanayakkara, A., Gonzales, C., Challacombe, M., Gill, P.M.W., Johnson, B., Chen, W., Wong, M.W., Andres, J.L., Gonzales, C., Head-Gordon, M., Replogle, E.S., Pople, J.A., 1998. Gaussian 98, Pittsburgh, PA.
[26] (a) T.S. Cameron, Z. Naturforsch. 32b (1977) 1001;
(b) T.S. Cameron, M.G. Magee, S. McLean, Z. Naturforsch. 31b (1976) 1295.
[27] (a) R.M. Badger, R.D. Waldron, J. Chem. Phys. 18 (1950) 566;
(b) R.M. Badger, R.D. Waldron, J. Chem. Phys. 26 (1957) 255;
(c) R. Mecke, W. Kutzelnigg, Spectrochim. Acta 16 (1960) 1215.
[28] T. Steiner, Angew. Chem. Int. Ed. 41 (2002) 48.